DOI: 10.1002/ejoc.200900818

3-(Pyridin-2-yl)[1,2,3]triazolo[1,5-*a*]quinoline: A Theoretical and Experimental Analysis of Ring-Chain Isomerisation

Rafael Ballesteros-Garrido,[a] Fernando Blanco,*[b] Rafael Ballesteros,*[c] Frédéric R. Leroux,*[a] Belén Abarca,*[c] Françoise Colobert,*[a] Ibon Alkorta,[b] and José Elguero[b]

Keywords: Heterocycles / Isomerization / Metalation / Density functional calculations

In the course of the synthesis of new fluorophores for molecular recognition an experimental (^{1}H NMR) and theoretical (DFT) study of the ring-chain isomerism of 3-(pyridin-2-yl)-[1,2,3]triazolo[1,5-*a*]quinoline derivatives (**A**) into 2-([1,2,3]-triazolo[1,5-*a*]pyridin-3-yl)quinoline derivatives (**B**) has been carried out. The rearrangement is influenced by steric and electronic effects of the substituents present on the quinoline ring.

Introduction

The chemistry of [1,2,3]triazolo[1,5-*a*]pyridines[1] includes the existence of ring-chain isomerism between the closed form of the triazole ring and the open form of the diazo compound.[2–4] Previously, some of us determined the mechanism of this ring-chain isomerism, both experimental and theoretically, in the case of substituted 3-(pyridin-2-yl)[1,2,3]triazolo[1,5-*a*]pyridines (**1**),[3] which indicated the existence of two different compounds: either **1A** or **1B** as depicted in Scheme 1.

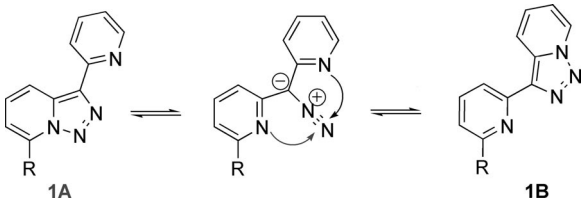

Scheme 1. Triazole ring-chain isomerisation.

[a] Laboratoire de Stéréochimie, CNRS, Université de Strasbourg (ECPM),
25 rue Becquerel, 67087 Strasbourg, France
Fax: +33-3-68-85-27-42
E-mail: frederic.leroux@unistra.fr
francoise.colobert@unistra.fr
[b] Instituto de Química Médica, CSIC,
Juan de la Cierva 3, 28006 Madrid, Spain
E-mail: fblanco@iqm.csic.es
[c] Departamento de Química Orgánica, Facultad de Farmacia, Universidad de Valencia,
Avda. Vicente Andrés Estellés s/n, 46100 Burjassot, Valencia, Spain
E-mail: belen.abarca@uv.es
Supporting information for this article is available on the WWW under http://dx.doi.org/10.1002/ejoc.200900818.

This equilibrium can be efficiently used for the preparation of 2,6-disubstituted pyridines[5,6] or of indolizines and imidazopyridines.[7] It is worth mentioning that such ring-chain isomerism is an important property of many heterocyclic systems.[8–10]

The ring-chain-ring isomerisation between structures **A** and **B** was found to be essentially dependent on the electronic properties of the R substituent. In general, **A**-type compounds are obtained with electron-donating substituents, whereas **B**-type compounds are formed with electron-withdrawing groups. Moreover, we have also shown how this isomerisation can be controlled by the presence of different phosphorus substituents (R = PX_2) bound to the triazolopyridine ring,[11] providing mixtures of **A**- and **B**-type structures in different proportions depending on the accepting/donating characters of the substituents on phosphorus (X).

We have quite recently reported on the fluorescence properties of compounds **1**.[12] We obtained good yields of various fluorescent tridentate ligands[13–15] that proved efficient in the detection of anions and cations.[16] From these results, we came to believe that it might be possible to develop new ligands with different electron densities as fluorescence sensors through the employment of the 3-(pyridin-2-yl)[1,2,3]triazolo[1,5-*a*]quinoline moiety, a benzo derivative of 3-(pyridin-2-yl)triazolopyridine, as fluorophore. So far, only some aspects of the synthesis and reactivity of [1,2,3]triazolo[1,5-*a*]quinolines have been reported by us and others.[17–20] Although 3-(pyridin-2-yl)[1,2,3]triazolo-[1,5-*a*]quinoline was a unknown compound, we believed that it should show an isomerisation equilibrium similar to that observed for triazolopyridine **1** (Scheme 2).

The ring-chain equilibrium should be governed by the substitution pattern on the condensed heterocyclic ring, similarly to what has been described in our work on tri-

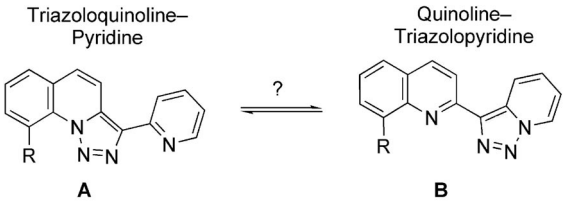

Scheme 2. Possible isomerisation of the triazoloquinoline–pyridine system.

azolopyridines.[3] To confirm this hypothesis, we synthesized a series of previously unknown triazoloquinolines (**2**–**13**, Scheme 5, below) in order to study the influence of different substituents on the ring-chain isomerisation and the relative position of the equilibrium. In parallel, theoretical calculations at the DFT/B3LYP/6–31G** level were performed to provide a better understanding of the isomerisation process and the different structures.

Results and Discussion

1) Synthesis and Properties of Triazoloquinoline–Pyridine/ Quinoline-Triazolopyridine Derivatives

The new triazoloquinoline–pyridine **2** was synthesized by a method similar to that described for the synthesis of the triazolopyridine–pyridine **1** (R = H).[21] (Pyridin-2-yl)(quinolin-2-yl)methanone was treated with hydrazine/methanol, and subsequent oxidation with MnO_2/chloroform afforded compound **2** in excellent yield (Scheme 3).

Typical ^{1}H NMR spectra of [1,2,3]triazolo[1,5-*a*]pyridines show characteristic coupling constants for the hydrogen at C7, adjacent to the nitrogen bridge of the triazolopyridine ring (doublet near 8.7 ppm, J_{H_6,H_7} = 6.9–7.1 Hz).[3]

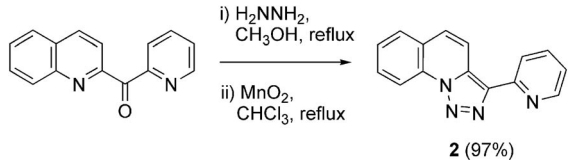

Scheme 3. Synthesis of triazoloquinoline–pyridine **2**.

This hydrogen can be clearly differentiated from a pyridine system hydrogen (broad doublet near 8.6 ppm, J_{H_2,H_3} = 4.7–5.1 Hz), as depicted in Figure 1. The triazoloquinoline structure also has a characteristic coupling constant, of J_{H_8,H_9} = 8 Hz.[17] By these criteria, NMR analysis of the new compound **2** allowed us to assign the pattern of signals to a pyridine–triazoloquinoline system (Scheme 2, structure **A**), without any traces of other secondary product.

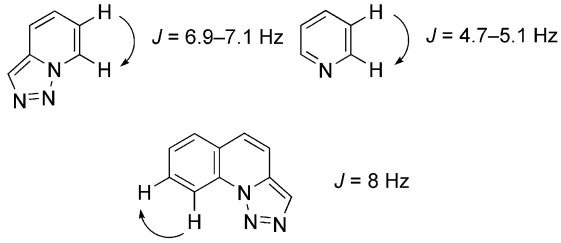

Figure 1. Typical ^{1}H NMR coupling constants.

The deuteration of 3-(pyridin-2-yl)[1,2,3]triazolo[1,5-*a*]-quinoline (**2A**), performed by deprotonation with butyllithium in THF at –78 °C and subsequent trapping of the lithio derivative with [D_4]methanol, also led exclusively to the isomer **3A** (Figure 2).

In contrast, when the same lithio derivative was quenched with iodine (Scheme 4), a ^{1}H NMR spectrum completely different from that of the deuterated analogue

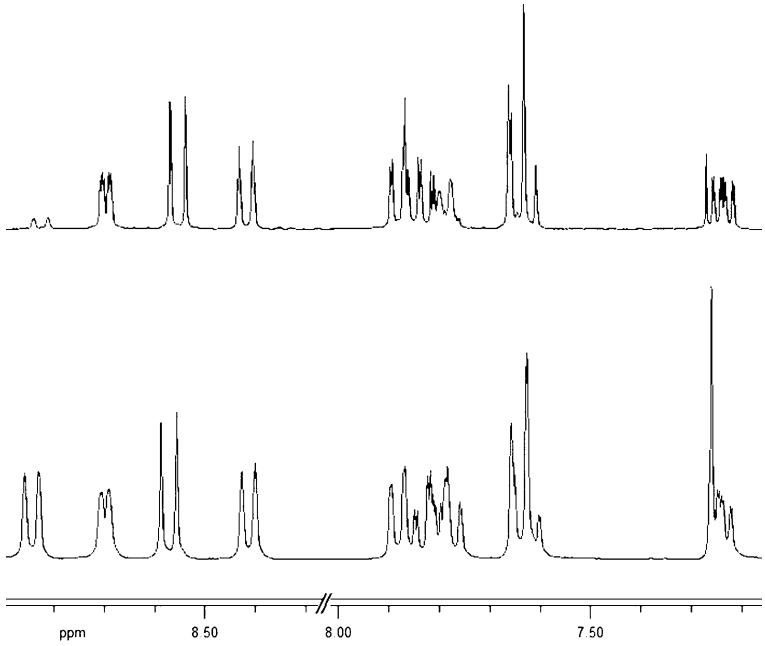

Figure 2. ^{1}H NMR of **2A** (below) and the corresponding deuterated compound **3A** (above). ^{9}H: δ = 8.86 ppm.

3A was obtained. The coupling constants indicated the exclusive presence of a quinoline–triazolopyridine system (Scheme 2, structure **B**). The structure of the new iodo derivative **4B** was confirmed by X-ray analysis of the compound (Figure 3).[22] The reversibility of this process was established by treatment of the iodinated compound **4B** with butyllithium in THF at –78 °C and trapping of the organometallic intermediate with methanol, which led exclusively to compound **2A** in 80% yield (Scheme 4).

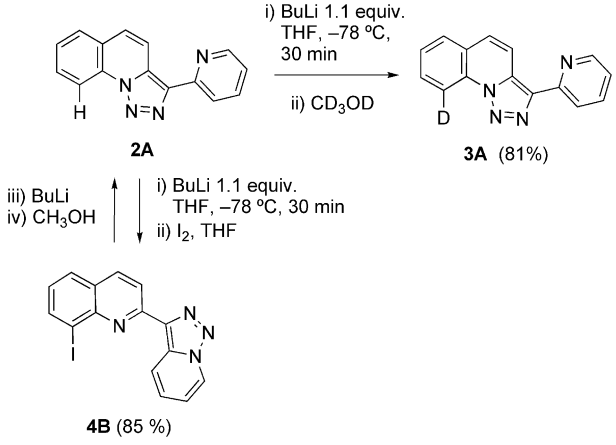

Scheme 4. Synthesis of triazoloquinoline **3A** and triazolopyridine **4B**.

In view of these results, we decided to prepare a series of new derivatives by metallation of **2** and treatment with different electrophiles (Scheme 5) in order to study the effects of the substitution. The lithiated intermediate was first quenched with iodomethane to afford the methyl derivative **5** (77%). Trapping with NFSI (*N*-fluorodibenzenesulfonimide) gave the fluorinated compound **6** in a yield of 50%. Fluorodimethoxyborane–diethyl ether as electrophile afforded alcohol **7** after addition of alkaline hydrogen peroxide, whereas borane **8** was obtained in good yield (79%) after quenching with 2-isopropoxy-4,4,5,5-tetramethyl-1,3,2-dioxaborolane. The methoxy derivative **9** was synthesized by methylation of alcohol **7** with methyl iodide in potassium carbonate (87%). The brominated compound **10** was obtained after trapping with 1,2-dibromo-1,1,2,2-tetrafluoroethane (73%) and the chlorinated quinoline **11** (62%) through the use of 1,2,2-trichloro-trifluoroethane. Carbinol **12** was obtained by quenching of the lithium intermediate with acetone (50%), and the alcohol **7** was also converted into the isopropyloxy derivative **13** by use of excess 2-bromopropane (80%). Unfortunately, all attempts to obtain a silylated derivative by trapping with different chlorotrialkylsilanes were unsuccessful, probably due to steric hindrance at the C9 position.

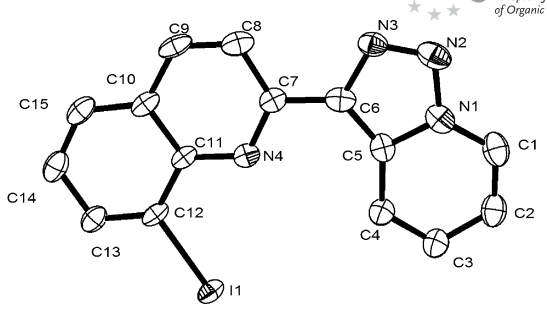

Figure 3. X-ray structure of **4B** (ORTEP plot).

As can be seen in Scheme 5, the structure of the final products, **A** or **B**, depend on the electronic and steric properties of the substituents. Moreover, some of the synthesized derivatives **5**, **6**, **9** and **13** were obtained as mixtures of both

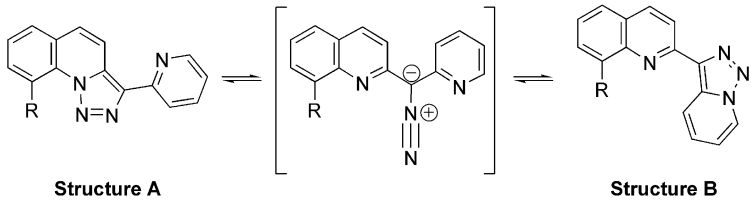

	Ratio [%]	
2A R = H	> 99 : 1	**2B** R = H
3A R = D	> 99 : 1	**3B** R = D
4A R = I	< 1 : 99	**4B** R = I
5A R = CH_3	52 : 48	**5B** R = CH_3
6A R = F	17 : 83	**6B** R = F
7A R = OH	> 99 : 1	**7B** R = OH
8A R = $B(OR)_2$ pinacol ester	> 99 : 1	**8B** R = $B(OR)_2$ pinacol ester
9A R = OCH_3	8 : 92	**9B** R = OCH_3
10A R = Br	< 1 : 99	**10B** R = Br
11A R = Cl	< 1 : 99	**11B** R = Cl
12A R = $C(OH)(CH_3)_2$	< 1 : 99	**12B** R = $C(OH)(CH_3)_2$
13A R = OiPr	15 : 85	**13B** R = OiPr

Scheme 5. Various triazoloquinoline derivatives obtained and their dependence on the nature of the substituent at C9. Ratios determined by ^1H NMR in $CDCl_3$.

Table 1. ^{1}H NMR spectroscopic data for compounds of type **A**.

Product	H4	H5	H6	H7	H8	H9	H3′	H4′	H5′	H6′	Other
2A	8.53 d J_1 = 9.3	7.6–7.5 m	7.9–7.8 m	7.6–7.5 m	7.9–7.8 m	8.86 d J_1 = 8.4	8.42 d J_1 = 8.0	7.9–7.8 m	7.24 dd J_1 = 7.4 J_2 = 4.9	8.70 br d J_1 = 4.9	
5A **A/B** 52:48	8.61 d J_1 = 9.3	7.62 d J_1 = 9.3	7.6–7.4 m	7.6–7.4 m	7.6–7.4 m	CH_3	8.41 ddd J_1 = 8.0 J_2 = 1.0 J_3 = 1.0	7.82 ddd J_1 = 8.0 J_2 = 7.8 J_3 = 1.0	7.24 ddd J_1 = 7.6 J_2 = 4.8 J_3 = 1.0	8.7 br d J_1 = 4.8 J_2 = 1.0 J_3 = 1.0	3.26 s CH_3
6A **A/B** 17:83	8.63 d J_1 = 9.4	7.7–7.4 m	7.7–7.4 m	7.7–7.4 m	7.7–7.4 m	F	8.42 br d J_1 = 8.0	7.81 app. td J_1 = 7.9 J_2 = 7.8 J_3 = 1.8	7.25 ddd J_1 = 7.7 J_2 = 4.8 J_3 = 1.1	8.68 d J_1 = 4.8	
7A	8.56 d J_1 = 9.4	7.70 d J_1 = 9.4	7.4–7.3 m	7.52 app. t J_1 = 7.9	7.4–7.3 m	OH	8.38 d J_1 = 8.0	7.86 apptd J_1 = 7.8 J_2 = 7.8 J_3 = 1.1	7.30 ddd J_1 = 7.5 J_2 = 4.8 J_3 = 1.1	8.73 br d J_1 = 4.8	10.71 s OH
8A	8.52 d J_1 = 9.3	7.53 d J_1 = 9.3	7.87 dd J_1 = 7.9 J_2 = 1.3	7.6–7.5 m	7.6–7.5 m	$B(OR)_2$ pinacol borane	8.38 ddd J_1 = 8.0 J_2 = 1.0 J_3 = 1.0	7.6–7.5 m	7.23 ddd J_1 = 7.5 J_2 = 4.9 J_3 = 1.0	8.70 ddd J_1 = 4.9 J_2 = 1.7 J_3 = 1.0	1.58 s 4 × CH_3
9A **A/B** 8:92	8.55 d J_1 = 9.3	7.6–7.4 m	7.30 dd J_1 = 7.9 J_2 = 1.3	7.6–7.4 m	7.6–7.4 m	OCH_3	8.34 J_1 = 7.9	7.6–7.4 m	7.3–72 m	8.60 m	4.18 s OCH_3
13A **A/B** 15:85	8.63 d J_1 = 9.3	7.51 d J_1 = 9.3	7.4–7.3 m	7.43 app. t J_1 = 7.8	7.4–7.3 m	O*i*Pr	8.44 ddd J_1 = 7.9 J_2 = 0.9 J_3 = 0.9	7.73 ddd J_1 = 7.9 J_2 = 7.8 J_3 = 1.8	7.15 ddd J_1 = 7.6 J_2 = 4.9 J_3 = 1.0	8.69 d J_1 = 4.9 J_2 = 1.7 J_3 = 0.9	4.74 sp A O*i*Pr J_1 = 6.1 1.58 d (A + B) O*i*Pr J_1 = 6.1

isomers with different ratios of distribution (see Tables 1 and 2). These results corroborate the existence of the isomeric equilibrium.

Tables 1 and 2 show the ^{1}H NMR spectroscopic data for all synthesized derivatives. The δ and J values for the most characteristic signals confirm that compounds **A** each constitute a triazoloquinoline–pyridine system, whereas compounds **B** each represent a quinoline–triazolopyridine structure.

A-Type Structures

As outlined in Figure 2, the unsubstituted derivative **2A** (R = H) shows four characteristic signals between δ = 8 and 9 ppm corresponding to the hydrogen atoms closest to the ring nitrogen (see indications for protons printed in grey in Figures 4 and 5). For all molecules belonging to the **A** series, the pyridine ring system could readily be characterized as reported in Table 1. All compounds of this series show similarities in the coupling constants and chemical shifts for the signals of H4A (8.5–8.6 ppm, J = 9.3–9.4 Hz) and H5A (7.5–7.6 ppm, J = 9.3–9.4 Hz), as well as for the pyridine hydrogen atoms H3′A and H6′A (columns 3′ and 6′ in Table 1).

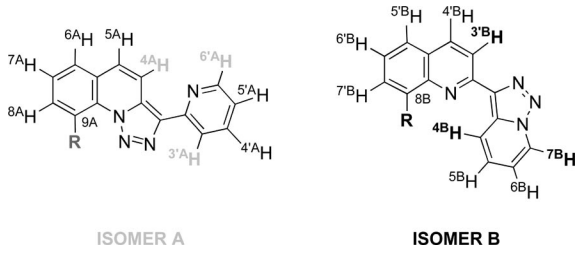

Figure 4. Proton assignment for **A**- (left) and **B**-type (right) isomers.

B-Type Structures

The same analysis as applied to the **A** series revealed similar ^{1}H NMR patterns for the quinoline proton H3′B (8.5–8.6 ppm, J_1 = 8.6–8.7). For all **B** systems studied the signals corresponding to the triazolopyridine ring could readily be characterized (H7B, H6B, H5B and H4B), with H4B being the most strongly down-shifted signal in all cases (proton indications printed in bold black, Figures 4 and 5, and Table 2). The chemical shift of the H4B proton proved to be very sensitive to the nature of the substituent R. This phenomenon can be associated with the geometry of the **B** structure, in which the two heterocyclic ring systems are oriented with the nitrogen atoms opposite to each other in order to avoid unfavourable repulsion between the nitrogen lone pairs. In this orientation, H4B points toward the lone pair of the quinoline ring nitrogen, and is close to the substituent R, so the proximity of H4B and R could explain the subtle influence of R on the shielding of H4B. This hypothesis was supported by analysis of the different halogenated derivatives. As can be seen in Table 2, there is a marked decrease in the chemical shift of H4B with decreasing halogen size: 9.43 ppm for the iodo compound **4B**, 9.29 ppm for the bromo derivative **10B** and 9.12 and 9.03 for the chloro- and fluoroquinolines **11B** and **6B**, respectively.

Table 2. ^{1}H NMR spectroscopic data for compounds of type **B**, where isolated.

Product	H3′	H4′	H5′	H6′	H7′	H8′	H4	H5	H6	H7	Other
4B	8.55 d	8.16 d	7.80 dd	7.22 app. t	8.31 dd	I	9.43 td	7.53 ddd	7.12 app. td	8.80 td	
	J_1 = 8.6	J_1 = 8.6	J_1 = 8.0	J_1 = 7.7	J_1 = 7.4		J_1 = 8.9	J_1 = 8.9	J_1 = 6.9	J_1 = 6.9	
			J_2 = 1.2		J_2 = 1.2		J_2 = 1.0	J_2 = 6.7	J_2 = 6.9	J_2 = 1.0	
							J_3 = 1.0	J_3 = 1.0	J_3 = 1.0	J_3 = 1.0	
5B	8.50 d	8.23 d	7.6–7.4 m	7.6–7.4 m	7.6–7.4 m	CH_3	8.98 ddd	7.48 ddd	7.12 app. td	8.83 ddd	2.93 s CH_3
A/B 52:48	J_1 = 8.6	J_1 = 8.6					J_1 = 8.9	J_1 = 8.9	J_1 = 6.9	J_1 = 7.0	
							J_2 = 1.0	J_2 = 6.7	J_2 = 6.9	J_2 = 1.0	
							J_3 = 1.0	J_3 = 1.0	J_3 = 1.0	J_3 = 1.0	
6B	8.56 d	8.24 dd	7.6–7.4 m	7.6–7.4 m	7.6–7.4 m	F	9.03 td	7.6–7.4 m	7.1 ddd	8.79 ddd	
A/B 17:83	J_1 = 8.7	J_1 = 8.7					J_1 = 8.9		J_1 = 6.9	J_1 = 7.0	
		J_2 = 1.2					J_2 = 1.0		J_2 = 6.8	J_2 = 1.0	
							J_3 = 1.0		J_3 = 1.0	J_3 = 1.0	
9B	8.52 d	8.21 d	7.07 d	7.5–7.4 m	7,5–7.4 m	OCH_3	9.03 td	7.48 m	7.10 app. td	8.79 ddd	4.14 s OCH_3
A/B 8:92	J_1 = 8.6	J_1 = 8.6	J_1 = 6,8				J_1 = 8.9	J_1 = 8.9	J_1 = 6.9	J_1 = 7.0	
							J_2 = 1.0	J_2 = 6.7	J_2 = 6.9	J_2 = 1.0	
							J_3 = 1.0	J_3 = 1.0	J_3 = 1.0	J_3 = 1.0	
10B	8.57 d	8.24 d	8.05 dd	7.36 app. t	7.79 dd	Br	9.29 td	7.54 ddd	7.13 ddd	8.81 ddd	
	J_1 = 8.6	J_1 = 8.6	J_1 = 7.5	J_1 = 7.8	J_1 = 8.0		J_1 = 8.9	J_1 = 8.9	J_1 = 6.9	J_1 = 7.0	
			J_2 = 1.2		J_2 = 1.2		J_2 = 1.0	J_2 = 6.7	J_2 = 6.8	J_2 = 1.0	
							J_3 = 1.0	J_3 = 1.0	J_3 = 1.0	J_3 = 1.0	
11B	8.58 d	8.26 d	7.84 dd	7.43 app. t	7.75 dd	Cl	9.21 td	7.54 ddd	7.13 ddd	8.81 ddd	
	J_1 = 8.6	J_1 = 8.6	J_1 = 7.5	J_1 = 7.8	J_1 = 8.1		J_1 = 8.9	J_1 = 8.9	J_1 = 6.9	J_1 = 7.0	
			J_2 = 1.2		J_2 = 1.2		J_2 = 1.0	J_2 = 6.7	J_2 = 6.8	J_2 = 1.0	
							J_3 = 1.0	J_3 = 1.0	J_3 = 1.0	J_3 = 1.0	
12B	8.62 d	8.33 d	7.70 dd	7.5–7.4 m	7.75 dd	C(OH)(CH_3)	8.80 ddd	7.56 ddd	7.12 ddd	8.83 ddd	8.35 s OH
	J_1 = 8.7	J_1 = 8.7	J_1 = 7.4		J_1 = 8.0		J_1 = 9.0	J_1 = 9.0	J_1 = 6.9	J_1 = 7.0	1.90 2 CH_3
			J_2 = 1.3		J_2 = 1.3		J_2 = 1.0	J_2 = 6.7	J_2 = 6.8	J_2 = 1.0	
							J_3 = 1.0	J_3 = 1.0	J_3 = 1.0	J_3 = 1.0	
13B	8.50 d	8.21 d	7.1–7.0 m	7.5–7.4 m	7.5–7.4 m	O*i*Pr	9.20 td	7.46 m	7.09 app. td	8.80 ddd	4.90 sp B O*i*Pr
A/B 15:85	J_1 = 8.6	J_1 = 8.6					J_1 = 8.9	J_1 = 8.9	J_1 = 6.9	J_1 = 7.1	J_1 = 6.0
							J_2 = 1.0	J_2 = 6.7	J_2 = 6.9	J_2 = 1.0	1.59 d (A + B) O*i*Pr
							J_3 = 1.0	J_3 = 1.0	J_3 = 1.0	J_3 = 1.0	J_1 = 6.1

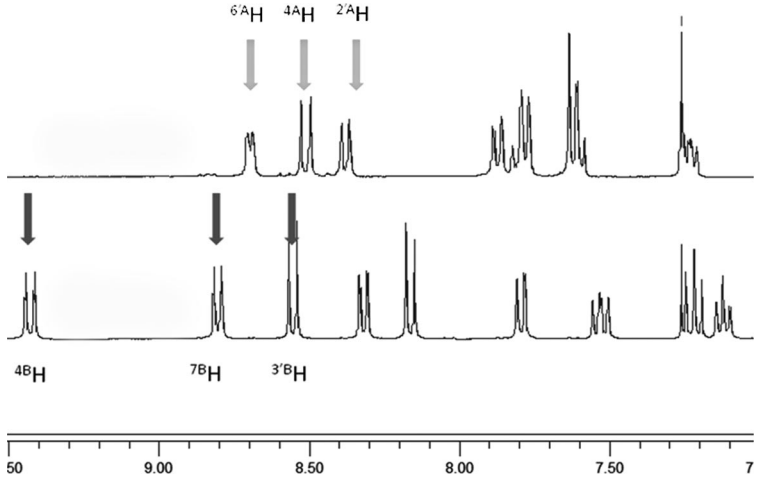

Figure 5. Aromatic regions of the ^{1}H NMR spectra of a representative structure **A** (**8A**, top) and a representative structure **B** (**4B**, bottom).

The experimental results so far showed the following characteristics:

1. As would be expected, electron-donating substituents favour structures of type **A**, whereas electron-accepting groups favour **B**-type structures. This observation is consistent with the case of the triazolopyridine–pyridine ring system **1**.

2. The ^{1}H NMR chemical shifts of H4A, H6′A, H3′A, H3′B, H4B and H7B, in chloroform, indicate that all systems feature *anti* orientations of the two heterocyclic subunits in order to avoid repulsive forces, as was confirmed by X-ray structural analysis (Figure 5).

3. If one considers only the electronic properties of substituents, the methyl derivative **5** should exist essentially as

the donor structure **5A**. The analogous 3-(pyridin-2-yl)[1,2,3]triazolo[1,5-*a*]pyridine system, for example, shows a **1A/1B** ratio of 75:25 in favour of the donor structure.[3] In contrast, the isomeric ratio found for the methyl derivative **5A/5B** (52:48) indicates that in the triazoloquinoline–pyridine ring systems steric effects must play an important role influencing the isomeric distribution (**A/B**). The structure **B** is sterically more favourable than the initial structure **A**.

4. We also studied the **5A/5B** equilibrium as a function of temperature and solvent. The initial ratio was not modified when the mixture was heated up to 65 °C (**A/B** 52:48). However, when the polarity of the solvent was changed ([D_6]acetone vs. [D_1]chloroform), an inversion of the isomeric distribution (**A/B** 41:59) was observed. The differences in the dipole moments of the two structures (**5A** and **5B**) as theoretically calculated are undoubtedly responsible for this behaviour.

2) Computational Studies

Two aspects of the structural behaviour of 3-(pyridin-2-yl)[1,2,3]triazolo[1,5-*a*]quinolines were studied computationally: the energetic profile of the isomerisation process for the unsubstituted derivative, and the isomer ratios of the **A/B** forms as a function of the substituents.

a) Reaction Profile (2, R = H)

Figure 6 shows the stationary points (minima and TSs) of the isomerisation reaction. The picture reveals an intricate process with several possible alternative pathways combining opening and rotational steps. We found eight local minima, four closed-ring (**M1**–**4**) and four open-chain (**M5**–**8**) isomers, and the subsequent transition states (**TSXY**). For the studied derivative (**2**, R = H), the global minimum corresponds to **M1**, the closed triazoloquinoline–pyridine isomer (**2A**), which is 14.9 kJ mol^{-1} more stable than **M3**, corresponding to the quinoline–triazolopyridine system (**2B**). The **M2** and **M4** minima are the rotational isomers of **M1** and **M3**, respectively, and are of lower stability, due to the repulsive effects explained in the next section. The open-chain minima **M5**–**8** show higher relative energy values.

Because of the complexity of the sequence, it is not easy to establish a single well-defined pathway to explain the equilibrium between the absolute minimum of each series (**M1** and **M3**). We therefore offer an explanation of the most likely situation by considering the route featuring the transition states with lower energy values. According to this criterion, we can see from the energetic diagram (Figure 7,

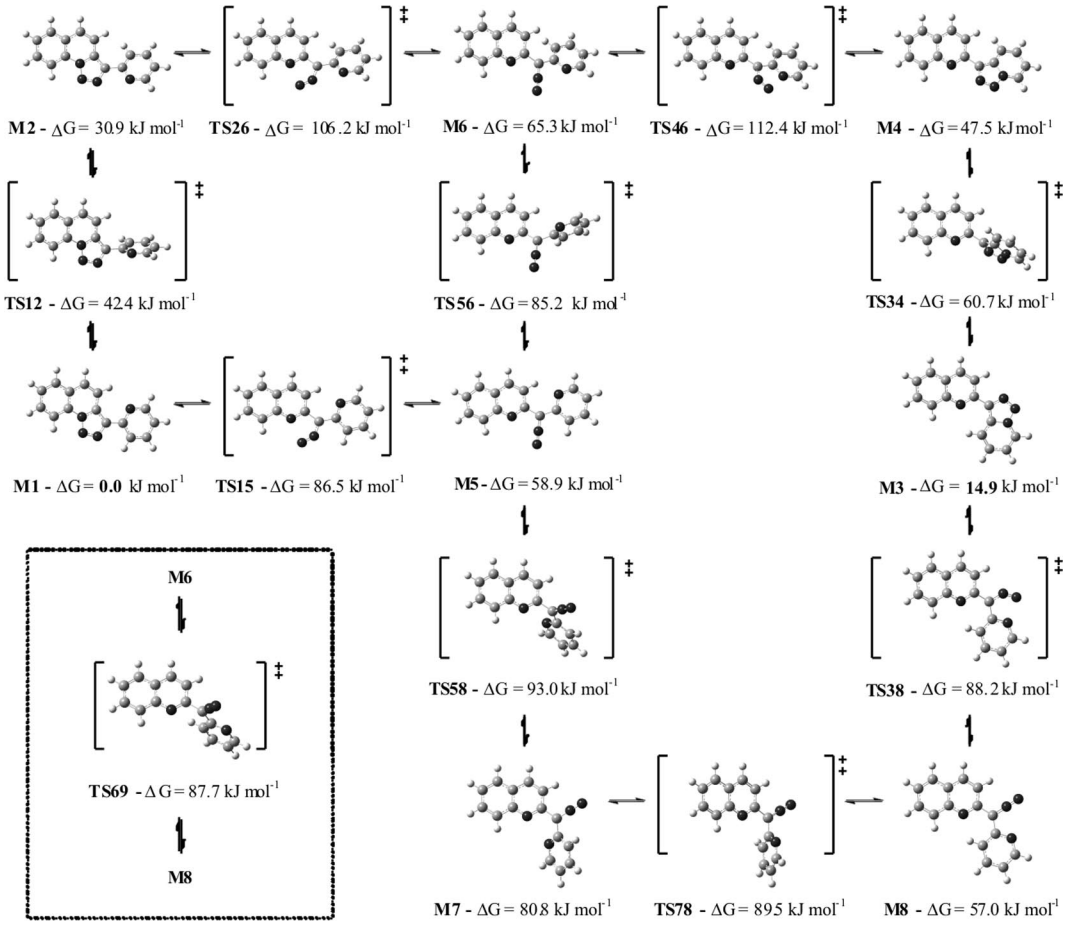

Figure 6. Stationary points (minima and TSs) of the isomerisation reaction for compound **2** (R = H).

pathway printed solid black) that the most favourable pathway from **M1** to **M3** proceeds by way of an initial opening step of **M1** through a planar **TS15** transition state, giving the **M5** intermediate, two consecutive rotational steps of the two heterocyclic rings over the diazo group (giving the **M6** and **M8** intermediates, respectively) and a final ring-closure step of **M8** to form the closed isomer **M3**. From **M5** to **M8** there is a second slightly less favourable pathway through the intermediate **M7** (Figure 7, pathway printed dashed black). Other possible sequences starting with a rotation of the ring from **M1** to **M2** pass through a second opening step with the significantly higher-energy-barrier transition state **TS26** (Figure 7, pathway printed in grey).

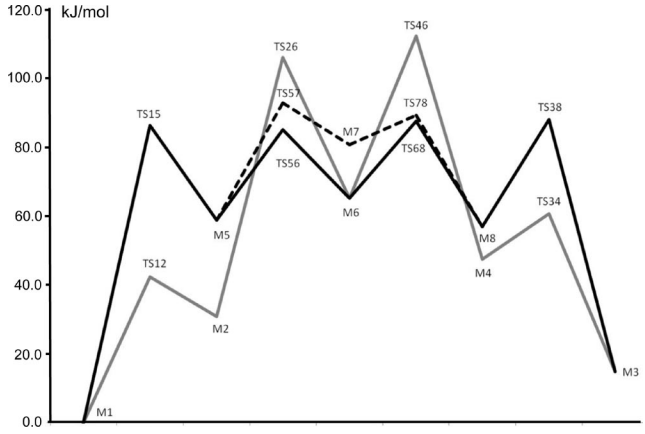

Figure 7. Energy diagram for the isomerisation reaction for compound **2** (R = H).

b) A/B Ratio (Computational Aspects)

In order to evaluate the effects of the substituents on the **A/B** ratio, different R groups, some of them corresponding to those obtained experimentally, were chosen for study. For all substituents the four closed isomers shown in Figure 8 were calculated.

Except in the case of R = Li, **A** and **B** are more stable than the corresponding rotamers **A′** and **B′**. Their geometries are more favourable because the repulsive effects between the nitrogen lone pairs and the proximal hydrogen atoms are avoided. In addition, these structures allow extra

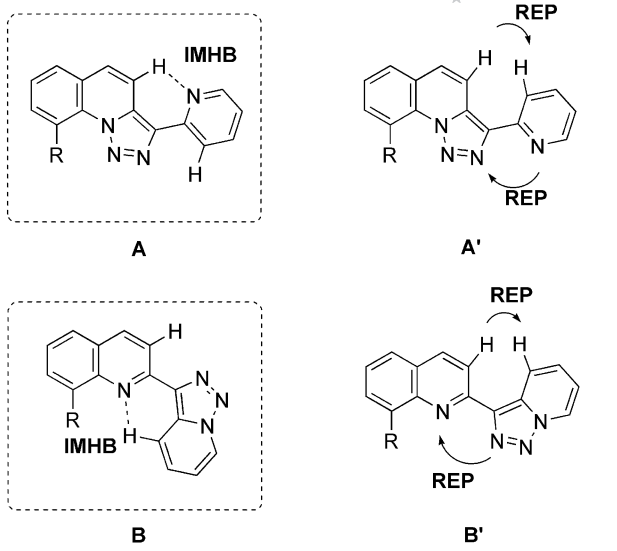

Figure 8. Structures of the isomers studied theoretically.

stabilization (Figure 9) arising from intramolecular hydrogen bonding (IMHB) either between H4A and the pyridine nitrogen (structure **A**) or between H4B and the quinoline nitrogen (structure **B**). These factors similarly explain the geometrical preference between the two heterocyclic ring systems. In general, the **A** and **B** structures adopt planar *anti* orientations, whereas the **A′** and **B′** structures should adopt torsional arrangements.

For certain cases [R = OH, CHO, OCH_3, NH_2, $N(CH_3)_2$] we evaluated a large number of structures with regard to the relative orientation of the substituent, because it could have an important influence on the final stability of the molecule, due to the possibility of creating attractive interactions by hydrogen bonding or repulsive ones between neighbouring atoms (Figure 10).

Table 3 shows the relative energies of the most stable configurations for each substituent considered. Negative values indicate that, for a given compound, the isomer **A** is favoured with respect to form **B** and the reverse applies for positive values. We can observe that the predictions deduced from the theoretical calculations are consistent with the experimental results.

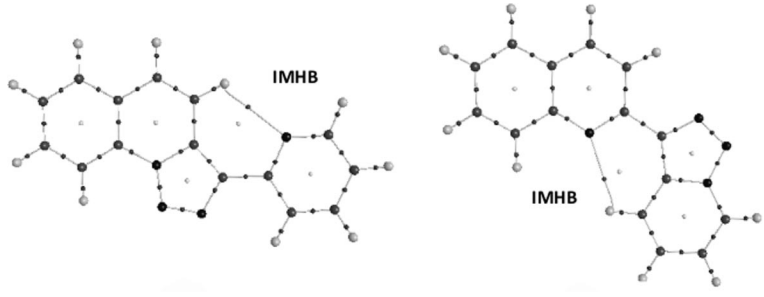

Figure 9. Molecular depiction of the electron density analysis of the structures **2A** (left) and **2B** (right). Bond and ring critical points are indicated and the lines connecting the atoms show the bond paths.

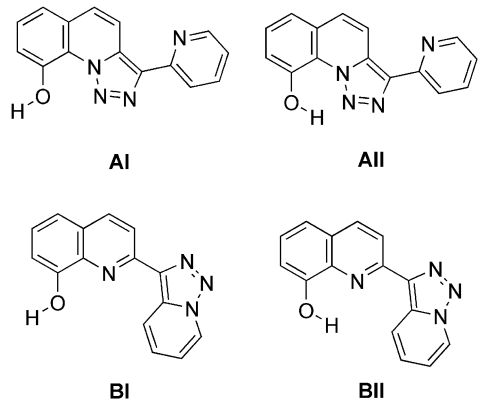

Figure 10. Structures studied as a function of the substituent orientation.

Table 3. Calculated **A/B** ratios for the derivatives (kJ mol^{-1}). The synthesized compounds are indicated with their corresponding numeration.

	R	ΔE	Theoretical	Experimentally determined **A/B** ratio
	Li	–66.11	**A**	–
	BH_2	–60.58	**A**	–
7	OH	–19.87	**A**	> 99:1
8	$B(OH)_2$	–16.25	**A**	> 99:1
2	H	–15.56	**A**	> 99:1
	NH_2	–15.54	**A**	–
	SiH_3	–9.66	**A**	–
	$Si(CH_3)_3$	–6.34	**A**	–
5	CH_3	–4.68	**A/B** mixture	52:48
	CHO	2.84	**A/B** mixture	–
6	F	3.70	**A/B** mixture	17:83
13	$OCH(CH_3)_2$	3.78	**A/B** mixture	15:85
9	OCH_3	5.02	**A/B** mixture	8:92
	NMe_2	7.06	**B**	–
12	$C(OH)(CH_3)_2$	14.90	**B**	< 1:99
11	Cl	16.98	**B**	< 1:99
	CN	17.96	**B**	–
4	I	19.95	**B**	< 1:99
	$C(CH_3)_3$	20.61	**B**	–
10	Br	21.28	**B**	< 1:99
	NO_2	21.84	**B**	–
	CF_3	22.08	**B**	–

General Trends

The electronic properties of the substituents play an essential role in the equilibria. The general trend is that electron-donating substituents stabilize the isomers of type **A** [R = Li (carbanion), BH_2, $B(OH)_2$, H, SiH_3, $Si(CH_3)_3$], whereas electron-accepting substituents stabilize the isomers of type **B** (R = CF_3, NO_2, Br, I, CN, Cl, NMe_2, OCH_3). This observation is consistent with the experimental results obtained in this work for the derivatives R = $B(OH)_2$, H, Cl, Br, I and is analogous with the isomerisation equilibria of 3-(pyridin-2-yl)[1,2,3]triazolo[1,5-*a*]pyridines.

In those cases in which the calculated energy difference between the two isomers was lower than 5 kJ mol^{-1} [CH_3, CHO, F, $OCH(CH_3)_2$ and OCH_3], the experimental results show mixtures of the two isomers. Furthermore, the experimental ratios were consistent with the sign of the value for the calculated energies. The energetic ratio calculated for the methyl derivative **5** (R = CH_3) is very low if we only take electronic criteria into consideration. Moreover, the parent compound **2** (R = H) clearly favours form **A**. This fact could be explained in terms of the influence of steric effects as outlined above.

The structures bearing halogen atoms follow the general criterion that structure type **B** is more favourable, due to their electronegativity. However, their stabilities (Br > I > Cl >> F) do not directly correlate with the electronegative characters of the halogens (F > Cl > Br > I). The **A/B** ratios are considerably more in favour of the **B** isomers in the cases of the bromo and iodo derivatives than in that of the fluorinated one. The formation of intramolecular hydrogen bonds together with possible steric factors might explain this order of stability. As shown in the graphical AIM analysis (Figure 11), in the cases of bromine and iodine, as a result of the geometries of the molecules and the electronic properties of the halogens, we can in each case observe an interaction between the halogen and the neighbouring hydrogen atom, creating a bifurcated hydrogen bond.[23] In the cases of chlorine and fluorine, this interaction is less pronounced, and insufficient to reflect a bond critical point (bcp) in the AIM analysis (Figure 11).

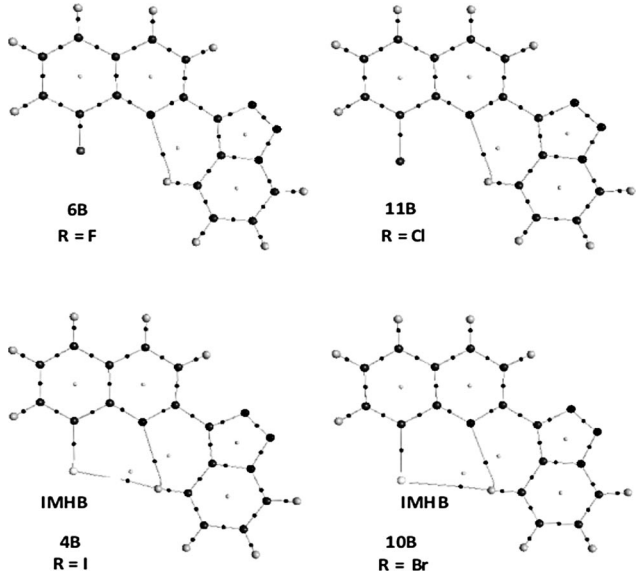

Figure 11. Molecular depiction of the electron density analysis of the halogenated derivatives. IMHB interaction between the halogen and H4B (**4B** and **10B**).

These IMHB interactions between the halogens and the proton H4B are reflected in the ^{1}H NMR spectra. Figure 12 shows how the signal corresponding to H4B is shifted significantly downfield from the fluoro derivative **6B** to the chloro (**11B**), bromo (**10B**) and iodo (**4B**) analogues. It is known that the interaction through the hydrogen bond pro-

duces a deshielding of the hydrogen involved.[24] As can be seen from Figure 12, for the series of halogenated compounds there is increasing deshielding of the H4B signal from fluorine to iodine, which could be due to increasing strength of the IMHB.

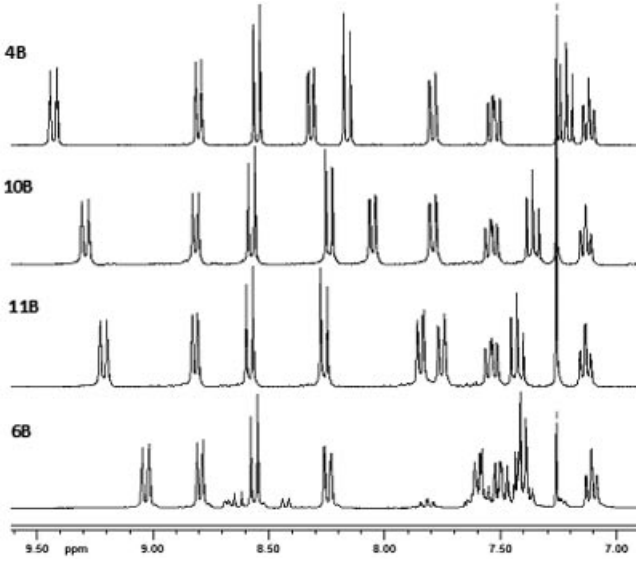

Figure 12. Comparison of the ^{1}H NMR spectra of the halogenated derivatives. From top to bottom: iodide **4B**, bromide **10B**, chloride **11B** and fluoride **6B**. The most strongly downfield-shifted signal corresponds to H4B.

Exceptions

The hydroxy derivative **7** shows a clear preference for the **A**-type structure, although because of the electronegativity of oxygen one might expect a preference for structure **B**. In fact, for this compound the relative orientation of the hydroxy substituent plays a crucial role. Structure **AII** in Figure 9 was found to be more stable than any of the **B** forms, because of the potential for IMHB between the OH group and the nitrogen atom N2 in the triazole ring. In contrast, the methoxy derivative **9**, with electronic characteristics similar to those of OH, but without the possibility of hydrogen bonding, favours the **B**-type isomer.

The computation studies predict a similar situation in the cases of R = NH_2 and R = $N(CH_3)_2$. The AIM analysis illustrates the presence of IMHB for these derivatives (Figure 13).

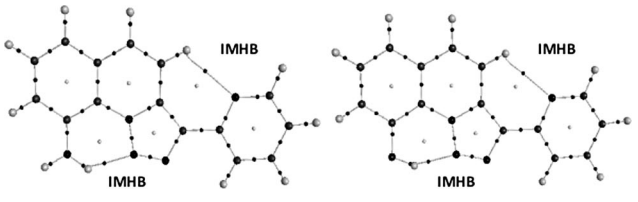

Figure 13. Molecular depiction of the electron density analysis of the **AII** isomers for R = OH (right) and NH_2 (left).

In the case of the carbinol **12** [R = $CHOH(CH_3)_2$, moderately electron-attracting], the only isomer obtained is isomer **B**, which is consistent with the computational studies. The AIM representation shows that isomer **B** experiences stabilizing interactions between the OH of the substituent, the nitrogen of the quinoline ring and the nearest H atoms of the adjacent heterocycles (Figure 14).

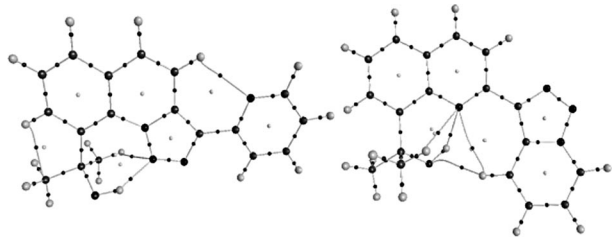

Figure 14. Molecular depiction of the electron density analysis of isomers **12A** (left) and **12B** (right).

According to the computational studies, the *tert*-butyl-substituted derivative shows a clear preference for the form **B**, for steric reasons, although form **A** should be more favourable because of its electron-donating properties (+I).

3) Triazolopyridine–Quinoline versus Triazoloquinoline–Pyridine

If we now compare the different triazolopyridine structures, we note that it is possible to modify the isomeric ratios of triazolopyridine–pyridines by introduction of a substituent into the 7-position (Scheme 6, first row), with the rearrangement leading to 2,6-disubstituted pyridines. Triazoloquinoline–pyridines undergo a similar rearrangement after introduction of substituents at the 9-position (Scheme 6, second row), analogously affording 2,8-disubstituted quinolines.[2,3] So far, however, we had not been able to modify the substitution pattern of the pyridine ring in a triazoloquinoline–pyridine in order to study which ring system governs the ring-chain isomerisation (Scheme 6, third row).

We therefore decided to prepare the derivatives **15** and **16** (Scheme 7), with C6′-brominated or C6′-methylated pyridine components in the triazoloquinoline–pyridine structure. The introduction of substituents onto triazoloquinoline **2A** by means of regioselective metallation at the C9-position and subsequent trapping with various electrophiles has been described.[20] Here, a new synthetic strategy was required. 2,6-Dibromopyridine was converted into ketone **14** in 70% yield after trapping of the monolithiated intermediate with methyl quinoline-2-carboxylate. Hydrazone formation and subsequent oxidation with MnO_2[21] afforded the bromo derivative **15**. Halogen/metal exchange and trapping with iodomethane gave the methylated derivative **16** in 50% yield (Scheme 7). Both 3-(6-bromopyridin-2-yl)[1,2,3]triazolo[1,5-*a*]quinoline (**15**) and 3-(6-methylpyridin-2-yl)[1,2,3]triazolo[1,5-*a*]quinoline (**16**) were exclusively obtained as form **A**.

These results can be interpreted in two ways: either in terms of the effect of the triazoloquinoline ring or in terms of the effect of the triazolopyridine ring.

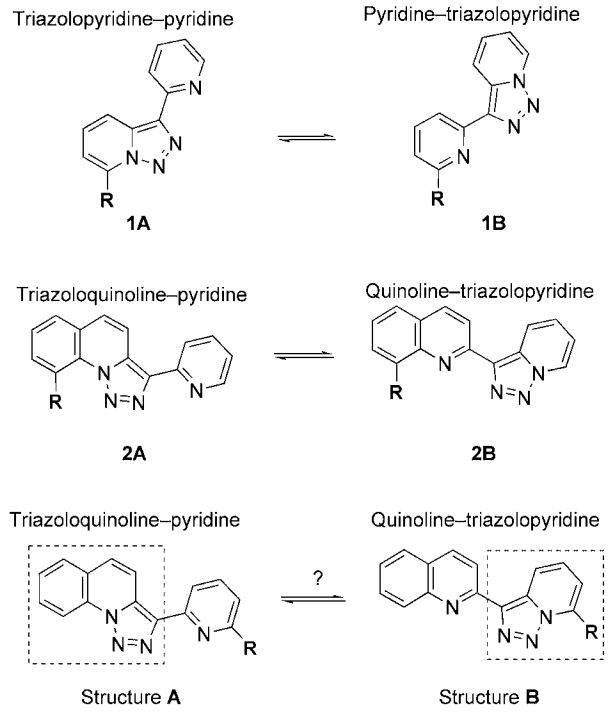

Scheme 6. Triazoloquinolines versus triazolopyridines.

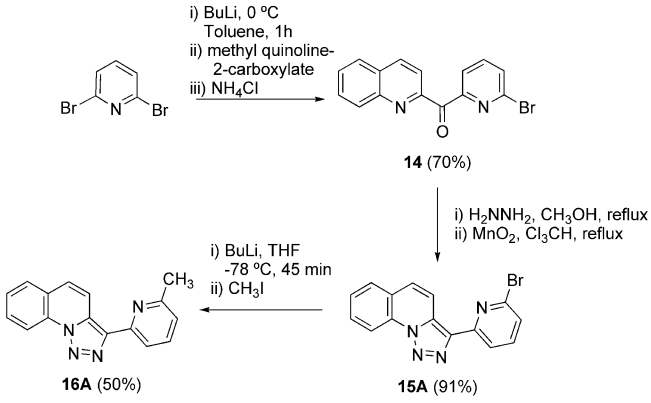

Scheme 7. Synthesis of the pyridyl-substituted compounds **15** and **16**.

The brominated derivative **15A** was obtained in the form that would be expected from both interpretations (i.e., the pyridine ring being the more electron-deficient heterocyclic subunit).

In contrast, the methylated derivative **16** gave a quite interesting result. If the triazoloquinoline–pyridine system is considered (Scheme 6, third row, structure **A**), the introduction of the methyl group on the pyridine ring should not have a significant influence on the equilibrium. In fact, according to the computational studies, the unsubstituted triazoloquinoline–pyridine structure **2** as form **A** is more stable than as form **B** (Table 3). If, however, we consider the quinoline–triazolopyridine system (Scheme 6, third row, structure **B**), the substitution of the triazolopyridine ring with an electron-donating methyl group should lead to the preferential form **B**, with the more electron-rich triazolopyridine subunit. Surprisingly, the only isomer obtained was **16A**, without any trace of **16B**. This experimental result indicates that: a) the contribution of the quinoline is more important than that of the pyridine component in the overall electronic situation of triazoloquinoline–pyridines, and b) stabilization of the **A** isomer, with a system of three condensed rings (triazoloquinoline), is stronger than the electron-donor effect of the methyl group in the triazolopyridine ring system of structure **B** (Figure 15). Calculations for compound **15** and **16** were consistent with the experimental results, showing higher stabilization of the **A** isomer in the two studied cases, though with significant differences of 41.90 and 9.27 kJ mol^{-1}, respectively.

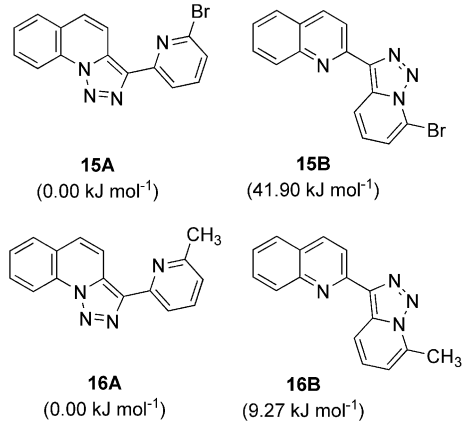

Figure 15. Relative energies of the two isomers of **15** and **16**.

Conclusions

A theoretical and experimental study of ring-chain isomerisation in new triazoloquinoline–pyridine systems has allowed us to explain the observed equilibrium ratios of the two possible ring-chain isomers **A** and **B** in terms of several effects of the substituents (hydrogen bonding, steric and electronic effects).

Experimental Section

General Methods: Starting materials, if commercially available, were purchased and used as such, provided that suitable checks (melting ranges, refractive indices and gas chromatography) had confirmed the claimed purity. When known compounds had to be prepared by literature procedures, pertinent references are given. Air- and moisture-sensitive materials were stored in Schlenk tubes. They were protected by and handled under argon, in appropriate glassware. Tetrahydrofuran was dried by distillation from sodium after the characteristic blue colour of sodium diphenyl ketyl (benzophenone-sodium "radical-anion") had been seen to persist. Ethereal or other organic extracts were dried by washing with brine and then by storage over sodium sulfate. Melting points or ranges (m.p.) given were determined on a Kofler heated stage and found to be reproducible after recrystallization, unless stated otherwise ("decomp."), and are uncorrected. If melting points are missing, this means all attempts to crystallize the liquid at temperatures down to –75 °C failed. Column chromatography was carried out on a

column packed with silica gel (60N spherical neutral size 63–210 μm). ^{1}H and (^{1}H decoupled) ^{13}C nuclear magnetic resonance (NMR) spectra were recorded at 400 or 300 and 101 or 75 MHz, respectively. Chemical shifts are reported in δ units, parts per million (ppm), and were measured relative to the signals for residual chloroform (δ = 7.27 ppm). Coupling constants (J) are given in Hz. Coupling patterns are abbreviated as, for example, s (singlet), d (doublet), t (triplet), q (quartet), quint (quintet), sp (septuplet), td (triplet of doublets), m (multiplet), app. s (apparent singlet) and br. (broad). COSY experiments were performed for all compounds. Only the major isomer is described in detail in the Experimental Section, but complete NMR assignment can be found in Tables 1 and 2.

Computational Details: Geometries of the stationary structures were fully optimized at the B3LYP theoretical level[25,26] with the 6-31G** basis set as implemented in the Gaussian 03 program.[27] Frequency calculations were carried out at the same computational level to confirm that all relevant structures correspond to energetic minima or real transition states. The electron densities in some of the systems were analysed by the Atoms In Molecules (AIM) methodology[28] with the AIM2000 package.[29]

3-(Pyridin-2-yl)[1,2,3]triazolo[1,5-*a*]quinoline (2): A mixture of (pyridin-2-yl)(quinolin-2-yl)methanone (3.5 g, 15 mmol, 1 equiv.) and hydrazine monohydrate (1.4 mL, 1.1 g, 22 mmol, 1.5 equiv.) in methanol (150 mL) was heated to reflux. The reaction was monitored by TLC until completion (3 h) and quenched with aqueous sodium hydroxide (20 mL, 30%). The resulting mixture was concentrated and extracted with dichloromethane (3 × 50 mL) The organic extracts were combined, washed with brine (20 mL), dried with sodium sulfate, filtered and concentrated to provide the corresponding hydrazone. The hydrazone was directly diluted in chloroform (150 mL). Activated manganese dioxide (3.7 g, 42 mmol, 2.8 equiv.) was added and the heterogeneous mixture was heated at reflux overnight. The resulting mixture was cooled to 25 °C and filtered over celite. After concentration, product **2** was obtained as a yellow solid (3.6 g, 97%); m.p. 157–158 °C. ^{1}H NMR (300 MHz, $CDCl_3$, 25 °C): δ = 8.86 (d, J = 8.4 Hz, 1 H, 9-H), 8.70 (d, J = 4.9 Hz, 1 H, 6′-H), 8.53 (d, J = 9.3 Hz, 1 H, 4-H), 8.42 (d, J = 8.0 Hz, 1 H, 3′-H), 7.9–7.8 (m, 3 H, 6-H, 8-H, 4′-H), 7.6–7.5 (m, 2 H, 5-H, 7-H), 7.24 (dd, J = 7.6, 4.9 Hz, 1 H, 5′-H) ppm. ^{13}C NMR (75.5 MHz, $CDCl_3$, 25 °C): δ = 151.9 (C), 149.2 (CH), 139.0 (C), 136.5 (CH), 131.7 (C), 129.9 (C), 129.8 (CH), 128.3 (CH), 127.3 (CH), 127.0 (CH), 124.2 (C), 122.0 (CH), 120.6 (CH), 117.7 (CH), 116.2 (CH) ppm. MS (EI): m/z (%) = 246 (11), 219 (15), 218 (100). HRMS (EI) for $C_{15}H_{10}N_4$: calcd. 246.0905; found 246.0899. $C_{15}H_{10}N_4$ (246.27): calcd. C 73.16, H 4.09, N 22.75; found C 72.89, H 4.30, N 22.89.

8-Iodo-2-([1,2,3]triazolo[1,5-*a*]pyridin-3-yl)quinoline (4): Butyllithium (0.5 mL, 0.5 mmol, 1.2 equiv.) in hexanes (1.5 M) was added dropwise at –78 °C to a solution of **2** (0.1 g, 0.4 mmol, 1.0 equiv.) in tetrahydrofuran (10 mL). The mixture was kept for 30 min at –78 °C, after which a solution of iodine (0.2 g, 0.5 mmol, 1.3 equiv.) in tetrahydrofuran (15 mL) was added, and the system was then allowed to reach 25 °C (1 h). The reaction mixture was hydrolysed with saturated aqueous sodium thiosulfate (20 mL). The resulting mixture was extracted with dichloromethane (3 × 50 mL). The organic extracts were combined, washed with brine (10 mL), dried with sodium sulfate, filtered and concentrated. Chromatography (silica gel, ethyl acetate/cyclohexane gradient) provided **4** as a white/yellow solid (0.12 g, 85%); m.p. 193–195 °C. ^{1}H NMR (300 MHz, $CDCl_3$, 25 °C): δ = 9.43 (td, J = 8.9, 1.0, 1.0 Hz, 1 H, 4-H), 8.80 (td, J = 6.9, 1.0, 1.0 Hz, 1 H, 7-H), 8.55 (d, J = 8.6 Hz, 1 H, 3′-H), 8.31 (dd, J = 7.4, 1.2 Hz, 1 H, 7′-H), 8.16 (d, J = 8.6 Hz, 1 H, 4′-H), 7.80 (dd, J = 8.0, 1.0 Hz, 1 H, 5′-H), 7.53 (ddd, J = 8.9, 6.7, 1.0 Hz, 1 H, 5-H), 7.22 (app. t, J = 7.7, Hz, 1 H, 6′-H), 7.12 (app. td, J = 6.9, 6.9, 1.0 Hz, 1 H, 6-H) ppm. ^{13}C NMR (75.5 MHz, $CDCl_3$, 25 °C): δ = 152.9 (C), 146.9 (C), 139.9 (CH), 137.3 (CH), 137.2 (C), 132.7 (C), 128.6 (CH), 127.9 (C), 127.4 (CH), 127.1 (CH), 125.2 (CH), 122.5 (CH), 119.6 (CH), 116.3 (CH), 103.3 (C) ppm. MS (EI): m/z (%) = 372 (24), 343 (83), 217 (100), 216 (42), 190 (25). HRMS (EI) for $C_{15}H_9IN_4$: calcd. 371.9872; found 371.9873.

2-([1,2,3]Triazolo[1,5-*a*]pyridin-3-yl)-8-methylquinoline (5B) and 9-Methyl-3-(pyridin-2-yl)[1,2,3]triazolo[1,5-*a*]quinoline (5A): Butyllithium (0.3 mL, 0.5 mmol, 1.2 equiv.) in hexanes (1.5 M) was added dropwise at –78 °C to a solution of **2** (0.1 g, 0.4 mmol, 1.0 equiv.) in tetrahydrofuran (10 mL). The mixture was kept for 30 min at –78 °C, after which a solution of iodomethane (68 mg, 0.5 mmol, 1.2 equiv.) in tetrahydrofuran (0.5 mL) was added, and the system was then allowed to reach 25 °C (1 h). Saturated aqueous ammonium chloride (20 mL) was added. The resulting mixture was extracted with dichloromethane (3 × 50 mL). The organic extracts were combined, washed with brine (10 mL), dried with sodium sulfate, filtered and concentrated. Chromatography (silica gel, ethyl acetate/cyclohexane, 3:2) allowed the isolation of two products. However, when NMR analysis was performed, both products revealed the same spectra, because they rapidly equilibrated between **5A** (52%) and **5B** (48%) with an **A/B** ratio of 1.0:0.9 (81 mg, 77%). ^{1}H NMR (300 MHz, $CDCl_3$, 25 °C): δ = 8.98 (td, J = 8.9, 1.2, 1.2 Hz, 1 H B, 4-H), 8.82 (td, J = 7.0, 1.0, 1.0 Hz, 1 H B, 7-H), 8.70 (td, J = 4.8, 1.0, 1.0 Hz, 1 H A, 6′-H), 8.61 (d, J = 9.3 Hz, 1 H A, 4-H), 8.54 (d, J = 8.6 Hz, 1 H B, 3′-H), 8.42 (td, J = 8.0, 1.0, 1.0 Hz, 1 H A, 3′-H), 8.23 (d, J = 8.6 Hz, 1 H B, 4′-H), 7.83 (dt, J = 7.9, 7.8, 1.8 Hz, 1 H A, 4′-H), 7.70 (app. t, J = 8.2, 8.2 Hz, 2 H), 7.65–7.56 (m, 2 H), 7.48 (ddd, J = 8.9, 6.7, 1.0 Hz, 1 H B, 5-H), 7.53–7.39 (m, 3 H), 7.25–7.23 (m, 1 H A, 5′-H), 7.11 (dt, J = 6.9, 6.9, 1.3 Hz, 1 H B, 6-H), 3.25 (s, 3 H A, CH_3), 2.93 (s, 3 H B, CH_3) ppm. ^{13}C NMR (75.5 MHz, $CDCl_3$, 25 °C): δ = 152.1 (C), 150.7 (C), 149.3 (CH), 148.7 (C), 147.0 (C), 138.1 (C), 137.5 (C), 136.7 (CH), 136.5 (CH), 136.4 (C), 133.1 (CH), 132.4 (C), 131.7 (C), 131.1 (C), 129.7 (CH), 128.6 (CH), 127.2 (C), 126.8 (CH), 126.4 (2×CH), 125.9 (C), 125.8 (2×CH), 125.3 (CH), 122.0 (CH), 121.5 (CH), 120.7 (CH), 118.5 (CH), 117.4 (CH), 115.9 (CH), 24.6 (CH_3), 18.467 (CH_3) ppm. MS (EI): m/z (%) = 260 (21), 232 (100), 231 (94). HRMS (EI) for $C_{16}H_{12}N_4$: calcd. 260.1062; found 260.1073.

8-Fluoro-2-([1,2,3]triazolo[1,5-*a*]pyridin-3-yl)quinoline (6B): Butyllithium (0.3 mL, 0.5 mmol, 1.2 equiv.) in hexanes (1.5 M) was added dropwise at –78 °C to a solution of **2** (0.1 g, 0.4 mmol, 1.0 equiv.) in tetrahydrofuran (10 mL). The mixture was kept for 30 min at –78 °C, after which a solution of *N*-fluorodibenzenesulfonimide (0.16 g, 0.5 mmol, 1.3 equiv.) in tetrahydrofuran (20 mL) was added, and the system was then allowed to reach 25 °C (1 h). A saturated aqueous ammonium chloride was added (20 mL) and the resulting mixture was extracted with dichloromethane (3 × 50 mL). The organic extracts were combined, washed with brine (10 mL), dried with sodium sulfate, filtered and concentrated. Preparative chromatography (silica 2 mm, ethyl acetate/cyclohexane, 1:3) provided **6B** as the major isomer as a slightly brown solid (70 mg, 50%). ^{1}H NMR (300 MHz, $CDCl_3$, 25 °C): δ = 9.03 (td, J = 8.9, 1.1, 1.1 Hz, 1 H, 4-H), 8.79 (td, J = 7.0, 0.9, 0.9 Hz, 1 H, 7-H), 8.56 (d, J = 8.7 Hz, 1 H, 3′-H), 8.24 (dd, J = 8.7, 1.2 Hz, 1 H, 4′-H), 7.6–7.4 (m, 4 H, 5-H, 5′-H, 6′-H, 7′-H), 7.10 (dt, J = 6.9, 6.8, 1.0 Hz, 1 H, 6-H) ppm. ^{13}C NMR (75.5 MHz, $CDCl_3$, 25 °C): δ = 158.1 (d, J = 256.3 Hz, 1 C), 152.0 (d, J = 1.4 Hz, 1 C), 149.3 (C),

137.0 (d, J = 51.0 Hz, 1 C), 136.1 (d, J = 3.1 Hz, CH), 132.8 (C), 128.8 (d, J = 2.3 Hz, 1 C), 127.3 (CH), 125.6 (d, J = 7.9 Hz, CH), 125.2 (CH), 123.3 (d, J = 4.6 Hz, CH), 121.8 (CH), 119.6 (CH), 116.3 (CH), 113.7 (d, J = 18.8 Hz, CH) ppm. MS (EI): m/z (%) = 264 (17), 236 (100), 216 (10), 190 (2). HRMS (EI) for $C_{15}H_9FN_4$: calcd. 264.0811; found 264.0816.

3-(Pyridin-2-yl)[1,2,3]triazolo[1,5-*a*]quinolin-9-ol (7): Butyllithium (1.4 mL, 2.2 mmol, 1.1 equiv.) was added at –78 °C to a solution of **2** (0.5 g, 2.0 mmol. 1.0 equiv.) in tetrahydrofuran (50 mL). The mixture was kept for 30 min at –78 °C, after which fluorodimethoxyborane–diethyl ether (0.6 mL, 2.7 mmol, 1.4 equiv.) was added, and the system was then allowed to reach 25 °C (1 h). After 30 min, aqueous sodium hydroxide (3.0 M , 0.8 mL) and aqueous hydrogen peroxide (30%, 0.2 mL) were added dropwise. The reaction mixture was kept at 25 °C during the night. After addition of saturated aqueous ammonium chloride (30 mL), the resulting mixture was extracted with dichloromethane (3 × 50 mL). The organic extracts were combined, washed with brine (10 mL), dried with sodium sulfate, filtered and concentrated. Chromatography (silica gel, ethyl acetate/cyclohexane, 1:3) provided **7** (430 mg, 82%); m.p. 158–159 °C. ^{1}H NMR (300 MHz, $CDCl_3$, 25 °C): δ = 10.71 (s, 1 H, OH), 8.73 (br. d, J = 4.8 Hz, 1 H, 6′-H), 8.56 (d, J = 9.4 Hz, 1 H, 4-H), 8.38 (d, J = 8.0 Hz, 1 H, 3′-H), 7.86 (app. td, J = 7.8, 7.8, 1.1 Hz, 1 H, 4′-H), 7.70 (d, J = 9.4 Hz, 1 H, 5-H), 7.52 (app. t, J = 7.9, 7.9 Hz, 1 H, 7-H), 7.4–7.3 (m, 2 H, 6-H, 8-H), 7.30 (ddd, J = 7.5, 4.8, 1.0 Hz, 1 H, 5′-H) ppm. ^{13}C NMR (75.5 MHz, $CDCl_3$, 25 °C): δ = 151.4 (C), 149.5 (CH), 148.8 (C), 138.2 (C), 136.7 (CH), 129.9 (C), 128.9 (CH), 128.2 (CH), 126.2 (C), 122.6 (CH), 120.8 (CH), 120.3 (C), 118.7 (CH), 117.4 (CH), 116.9 (CH) ppm. MS (EI): m/z (%) = 262 (33), 234 (100), 218 (19), 206 (48), 205 (65). HRMS (EI) for $C_{15}H_{10}N_4O$: calcd. 262.0855; found 262.0853. $C_{15}H_{10}N_4O$ (262.27): calcd. C 68.69, H 3.84, N 21.31; found C 68.51, H 4.02, N 21.47.

3-(Pyridin-2-yl)-9-(4,4,5,5-tetramethyl-1,3,2-dioxaborolan-2-yl)-[1,2,3]triazolo[1,5-*a*]quinoline (8): Butyllithium (0.6 mL, 1.0 mmol, 1.2 equiv.) in hexanes (1.5 M) was added dropwise at –78 °C to a solution of **2** (0.2 g, 0.8 mmol, 1.0 equiv.) in tetrahydrofuran (20 mL). The mixture was kept for 30 min at –78 °C, after which 2-isopropoxy-4,4,5,5-tetramethyl-1,3,2-dioxaborolane (0.2 mL, 0.2 g, 1.4 mmol, 1.3 equiv.) was added, and the system was then allowed to reach 25 °C (1 h). Saturated aqueous ammonium chloride (20 mL) was added. The resulting mixture was extracted with dichloromethane (3 × 50 mL). The organic extracts were combined, washed with brine (10 mL), dried with sodium sulfate, filtered and concentrated. Chromatography (silica gel, ethyl acetate/cyclohexane, 1:1) provided **8** as a colourless solid (0.2 g, 79%); m.p. 142–143 °C. ^{1}H NMR (300 MHz, $CDCl_3$, 25 °C): δ = 8.70 (ddd, J = 4.9, 1.7, 1.0 Hz, 1 H, 6′-H), 8.52 (d, J = 9.3 Hz, 1 H, 4-H), 8.38 (td, J = 8.0, 1.0, 1.0 Hz, 1 H, 3′-H), 7.87 (dd, J = 7.9, 1.3 Hz, 1 H, 6-H), 7.53 (d, J = 9.3 Hz, 1 H, 5-H), 7.6–7.5 (m, 3 H, 4′-H, 7-H, 8-H), 7.23 (ddd, J = 7.5, 4.9, 1.0 Hz, 1 H, 5′-H), 1.58 (s, 12 H, 4×CH_3) ppm. ^{13}C NMR (75.5 MHz, $CDCl_3$, 25 °C): δ = 151.9 (C), 149.2 (CH, 1 C), 139.0 (C), 136.7 (CH), 134.0 (CH), 133.2 (C), 130.0 (C), 129.2 (CH), 127.9 (CH), 126.7 (CH), 123.9 (C), 122.1 (CH), 120.9 (CH), 117.5 (CH), 84.810 (2×C), 25.012 (4×CH_3) ppm. MS (EI): m/z (%) = 371 (6), 345 (23), 344 (100),343 (25) 314 (23), 285 (28), 245 (77), 244 (58), 218 (47). HRMS (EI) for $C_{21}H_{21}BN_4O_2$: calcd. 371.1794; found 371.1789. $C_{21}H_{21}BN_4O_2$ (372.23): calcd. C 67.76, H 5.69, N 15.05; found C 67.60, H 5.69, N 15.55.

8-Methoxy-2-([1,2,3]triazolo[1,5-*a*]pyridin-3-yl)quinoline (9B): A mixture of **8** (60 mg, 0.23 mmol, 1 equiv.), iodomethane (42 mg, 0.3 mmol, 1.2 equiv.) and potassium carbonate (39 mg, 0.3 mmol, 1.3 equiv.) in acetone (20 mL) was heated to reflux. The reaction was monitored by TLC until completion (5 h). The reaction mixture was quenched with water (10 mL), and the resulting mixture was concentrated and then extracted with dichloromethane (3 × 10 mL) The organic extracts were combined, washed with brine (20 mL), dried with sodium sulfate, filtered and concentrated to provide **9B** as the major isomer (54 mg, 87%). ^{1}H NMR (300 MHz, $CDCl_3$, 25 °C): δ = 9.03 (td, J = 8.9, 1.2, 1.2 Hz, 1 H, 4-H), 8.79 (ddd, J = 7.0, 1.0, 1.0 Hz, 1 H, 7-H), 8.52 (d, J = 8.6 Hz, 1 H, 3′-H), 8.21 (d, J = 8.6 Hz, 1 H, 4′-H), 7.48 (ddd, J = 8.9, 6.7, 1.0 Hz, 1 H, 5-H), 7.5–7.4 (m, 2 H, 6′-H, 7′-H), 7.10 (app. td, J = 6.9, 6.9, 1.0 Hz, 1 H, 6-H), 7.07 (d, J = 6.8 Hz, 1 H, 5′-H), 4.14 (s, 3 H, OCH_3) ppm. ^{13}C NMR (75.5 MHz, $CDCl_3$, 25 °C): δ = 155.4 (C), 150.8 (C), 149.2 (C), 139.9 (C), 136.6 (C), 136.5 (CH), 128.4 (C), 127.0 (CH), 126.2 (CH), 125.2 (CH), 121.8 (CH), 119.7 (CH), 119.3 (CH), 116.1 (CH), 108.2 (CH), 56.2 (CH_3) ppm. MS (EI): m/z (%) = 276.1 (30), 248.1 (50), 218.1 (70), 218 (100), 141.9 (85). HRMS (EI) calcd. for $C_{16}H_{12}N_4O$ [M + H]: 277.1084; found 277.1050. HRMS (EI) calcd. for [M + Li] 283.1166; found 283.1130.

8-Bromo-2-([1,2,3]triazolo[1,5-*a*]pyridin-3-yl)quinoline (10): Butyllithium (0.3 mL, 0.5 mmol, 1.2 equiv.) in hexanes (1.5 M) was added dropwise at –78 °C to a solution of **2** (0.1 g, 0.4 mmol, 1.0 equiv.) in tetrahydrofuran (10 mL). The mixture was kept for 30 min at –78 °C, after which a solution of 1,2-dibromo-1,1,2,2-tetrafluoroethane (0.2 g, 0.5 mmol, 1.3 equiv.) in tetrahydrofuran (1 mL) was added, and the system was then allowed to reach 20 °C (1 h). Saturated aqueous ammonium chloride (20 mL) was added. The resulting mixture was extracted with dichloromethane (3 × 50 mL) and the organic extracts were combined, washed with brine (10 mL), dried with Na_2SO_4, filtered and concentrated. Chromatography (silica gel, ethyl acetate/cyclohexane gradient) provided **10** as a slightly yellow solid (95 mg, 73%); m.p. 231–233 °C. ^{1}H NMR (300 MHz, $CDCl_3$, 25 °C): δ = 9.29 (td, J = 8.9, 1.0, 1.0 Hz, 1 H, 4-H), 8.81 (td, J = 7.0, 1.0, 1.0 Hz, 1 H, 7-H), 8.57 (d, J = 8.6 Hz, 1 H, 3′-H), 8.24 (d, J = 8.6 Hz, 1 H, 4′-H), 8.05 (dd, J = 7.5, 1.2 Hz, 1 H, 5′-H), 7.79 (dd, J = 8.0, 1.2 Hz, 1 H, 7′-H), 7.54 (ddd, J = 8.9, 6.7, 1.0 Hz, 1 H, 5-H), 7.36 (app. t, J = 7.8 Hz, 1 H, 6′-H), 7.13 (ddd, J = 6.9, 6.8, 1.0 Hz, 1 H, 6-H) ppm. ^{13}C NMR (75.5 MHz, $CDCl_3$, 25 °C): δ = 152.8 (C), 145.0 (C), 137.4 (C), 137.0 (CH), 133.1 (CH), 132.9 (C), 128.5 (C), 127.6 (CH), 127.5 (CH), 126.4 (CH), 125.3 (CH), 124.9 (C), 122.1 (CH), 119.5 (CH), 116.3 (CH) ppm. MS (EI): m/z (%) = 326 (16), 324 (15), 298 (85), 295 (82), 217 (100), 216 (81), 190 (41). HRMS (EI) calcd. for $C_{15}H_9{}^{79}BrN_4$: 324.0011; found 323.9971. HRMS (EI) calcd. for $C_{15}H_9{}^{81}BrN_4$: calcd. 326.0011; found 325.9985.

8-Chloro-2-([1,2,3]triazolo[1,5-*a*]pyridin-3-yl)quinoline (11): Butyllithium (0.3 mL, 0.5 mmol, 1.2 equiv.) in hexanes (1.5 M) was added dropwise at –78 °C to a solution of **2** (0.1 g, 0.4 mmol, 1.0 equiv.) in tetrahydrofuran (10 mL). The mixture was kept for 30 min at –78 °C, after which a solution of 1,2,2-trichlorotrifluoroethane (0.07 mL, 0.1 g, 0.5 mmol, 1.3 equiv.) in tetrahydrofuran (1 mL) was added, and the system was then allowed to reach 25 °C (1 h). Saturated aqueous ammonium chloride (20 mL) was added and the resulting mixture was extracted with dichloromethane (3 × 50 mL). The organic extracts were combined, washed with brine (10 mL), dried with sodium sulfate, filtered and concentrated. Chromatography (silica gel, ethyl acetate/cyclohexane, 3:2) provided **11** as a light brown solid (70 mg, 62%); m.p. 228–230 °C. ^{1}H NMR (300 MHz, $CDCl_3$, 25 °C): δ = 9.21 (td, J = 8.9, 1.0, 1.0 Hz, 1 H, 4-H), 8.81 (td, J = 7.0, 1.0, 1.0 Hz, 1 H, 7-H), 8.58 (d, J = 8.6 Hz, 1 H, 3′-H), 8.26 (d, J = 8.6 Hz, 1 H, 4′-H), 7.84 (dd, J = 7.5,

1.2 Hz, 1 H, 5′-H), 7.75 (dd, *J* = 8.1, 1.2 Hz, 1 H, 7′-H), 7.54 (ddd, *J* = 8.9, 6.7, 1.0 Hz, 1 H, 5-H), 7.43 (t, *J* = 7.8 Hz, 1 H, 6′-H), 7.13 (ddd, *J* = 6.9, 6.8, 1.0 Hz, 1 H, 6-H) ppm. ^{13}C NMR (75.5 MHz, $CDCl_3$, 25 °C): δ = 152.5 (C), 144.2 (C), 137.5 (C), 136.9 (CH), 133.4 (C), 133.0 (C), 129.6 (CH), 128.5 (C), 127.5 (CH), 126.8 (CH), 125.9 (CH), 125.3 (CH), 122.0 (CH), 119.5 (CH), 116.3 (CH) ppm. MS (EI): *m*/*z* (%) = 282 (4), 280 (15), 254 (31), 252 (100), 217 (35), 216 (31), 190 (16). HRMS (EI) calcd. for $C_{15}H_9{}^{35}ClN_4$: 280.0516; found 280.0508. HRMS (EI) calcd. for $C_{15}H_9{}^{37}ClN_4$: 282.0516; found 282.0510.

2-[2-([1,2,3]Triazolo[1,5-*a*]pyridin-3-yl)quinolin-8-yl]propan-2-ol (12): Butyllithium (0.3 mL, 0.5 mmol, 1.2 equiv.) in hexanes (1.5 M) was added dropwise at –78 °C to a solution of **2** (0.1 g, 0.4 mmol, 1.0 equiv.) in tetrahydrofuran (10 mL). The mixture was kept for 30 min at –78 °C, after which acetone (1 mL, excess) was added, and the system was then allowed to reach 25 °C (1 h). Saturated aqueous ammonium chloride (20 mL) was added and the resulting mixture was extracted with dichloromethane (3 × 50 mL). The organic extracts were combined, washed with brine (10 mL), dried with sodium sulfate, filtered and concentrated. Chromatography (silica gel, ethyl acetate/cyclohexane, 1:3) provided **12** as a colourless solid (60 mg, 50%); m.p. 131–133 °C. ^{1}H NMR (300 MHz, $CDCl_3$, 25 °C): δ = 8.83 (ddd, *J* = 7.0, 1.0, 1.0 Hz, 1 H, 7-H), 8.80 (ddd, *J* = 9.0, 1.0, 1.0 Hz, 1 H, 4-H), 8.62 (d, *J* = 8.7 Hz, 1 H, 3′-H), 8.35 (br. s, 1 H, OH), 8.33 (d, *J* = 8.7 Hz, 1 H, 4′-H), 7.75 (dd, *J* = 8.0, 1.4 Hz, 1 H, 7′-H), 7.70 (dd, *J* = 7.4, 1.4 Hz, 1 H, 5′-H), 7.56 (ddd, *J* = 8.9, 6.7, 1.0 Hz, 1 H, 5-H), 7.5–7.4 (m, 1 H, 6′-H), 7.12 (ddd, *J* = 6.9, 6.8, 1.2 Hz, 1 H, 6-H), 1.90 (s, 6 H, 2×CH_3) ppm. ^{13}C NMR (75.5 MHz, $CDCl_3$, 25 °C): δ = 149.6 (C), 145.8 (C), 143.7 (C), 138.3 (CH), 137.0 (C), 131.9 (C), 128.2 (C), 128.0 (CH), 127.3 (CH), 126.1 (CH), 126.1 (CH), 125.8 (CH), 119.8 (CH), 119.3 (CH), 116.1 (CH), 74.3 (C), 31.2 (2 CH_3) ppm. MS (EI): *m*/*z* (%) = 304 (2), 290 (12), 289 (60), 276 (36), 262 (19), 261 (100), 257 (35), 243 (58), 242 (26), 233 (16), 219 (24), 190 (11). HRMS (EI) for $C_{18}H_{16}N_4O$: calcd. 304.1324; found 304.1321.

2-([1,2,3]Triazolo[1,5-*a*]pyridin-3-yl)-8-isopropoxyquinoline (13B): A mixture of **7** (60 mg, 0.23 mmol, 1 equiv.), 2-bromopropane (0.3 g, 2.3 mmol, 10 equiv.) and potassium carbonate (39 mg, 0.3 mmol, 1.3 equiv.) in acetone (20 mL) was heated to reflux. The reaction was monitored by TLC until completion (24 h). The reaction mixture was quenched with water (10 mL), concentrated and extracted with dichloromethane (3 × 10 mL) The organic extracts were combined, washed with brine (20 mL), dried with sodium sulfate, filtered and concentrated to provide **13B** as the major isomer (59 mg, 85%). ^{1}H NMR (300 MHz, $CDCl_3$, 25 °C): δ = 9.20 (td, *J* = 8.9, 1.0, 1.0 Hz, 1 H, 4-H), 8.80 (ddd, *J* = 7.1, 1.0, 1.0 Hz, 1 H, 7-H), 8.50 (d, *J* = 8.6 Hz, 1 H, 3′-H), 8.21 (d, *J* = 8.6 Hz, 1 H, 4′-H), 7.5–7.4 (m, 2 H, 6′-H, 7′-H) 7.46 (ddd, *J* = 8.9, 6.7, 1.0 Hz, 1 H, 5-H), 7.09 (app. td, *J* = 6.9, 6.9, 1.0 Hz, 1 H, 6-H), 7.1–7.0 (m, 1 H, 5′-H), 4.90 (sp, *J* = 6.0 Hz, 1 H, OCH), 1.59 (d, *J* = 6.0 Hz, 6 H, 2×CH_3) ppm. ^{13}C NMR (75.5 MHz, $CDCl_3$, 25 °C): δ = 153.7 (C), 140.69 (C), 138.2 (C), 139.9 (C), 136.4 (CH), 132.8 (C) 128.6 (C), 126.7 (CH), 126.2 (CH), 125.2 (CH), 122.1 (CH), 119.7 (CH), 118.8 (CH), 116.1 (CH), 111.8 (CH), 71.1 (CH), 22.3 (2×CH_3) ppm. MS (EI): *m*/*z* (%) = 304 (17), 289 (16), 276 (69), 235 (22), 234 (100), 218 (30) 206 (36), 205 (62), 78 (10). HRMS (EI) calcd. for $C_{18}H_{16}N_4O$: 304.1324; found 304.1316,

(6-Bromopyridin-2-yl)(quinolin-2-yl)methanone (14): Butyllithium (10.8 mL, 16.7 mmol, 1.1 equiv.) in hexanes (1.5 M) was added dropwise at 0 °C to a solution of 2,6-dibromopyridine (3.6 g, 15.2 mmol, 1.1 equiv.) in toluene (75 mL). The mixture was kept for 20 min at 0 °C before cannulation into a solution of methyl quinoline-2-carboxylate (2.8 g, 14.9 mmol, 1.0 equiv.) in tetrahydrofuran (100 mL) at 0 °C. The mixture was allowed to reach 25 °C in the course of 1 h and hydrolysed with saturated aqueous ammonium chloride (20 mL). The resulting mixture was extracted with dichloromethane (3 × 50 mL). The organic extracts were combined, washed with brine (3 × 10 mL), dried with sodium sulfate, filtered and concentrated. Chromatography (silica gel, ethyl acetate/cyclohexane, 1:2) provided **14** as a yellow oil (3.3 g, 70%). ^{1}H NMR (300 MHz, $CDCl_3$, 25 °C): δ = 8.32 (d, *J* = 8.5 Hz, 1 H, 3-H), 8.2–8.1 (m, 3 H), 7.88 (dd, *J* = 8.1, 1.2 Hz, 1 H), 7.8–7.7 (m, 2 H), 7.7–7.60 (m, 1 H) ppm. ^{13}C NMR (75.5 MHz, $CDCl_3$, 25 °C): δ = 191.2 (C), 154.9 (C), 153.3 (C), 147.1 (C), 141.8 (C), 138.6 (CH), 136.8 (CH), 130.9 (CH), 130.6 (CH), 130.1 (CH), 129.1 (C), 128.7 (CH), 127.6 (CH), 124.7 (CH), 120.8 (CH) ppm. MS (EI): *m*/*z* (%) = 314 (63), 312 (65), 286 (34), 285 (55), 284 (31), 283 (51), 205 (71), 128 (100), 101 (29). HRMS (EI) calcd. for $C_{15}H_9{}^{79}BrN_2$: 311.9898; found 311.9892. HRMS (EI) calcd. for $C_{15}H_9{}^{81}BrN_2$: 313.9898; found 313.9882.

3-(6-Bromopyridin-2-yl)[1,2,3]triazolo[1,5-*a*]quinoline (15): A mixture of (6-bromopyridin-2-yl)-(quinolin-2-yl)methanone (1.0 g, 3.3 mmol, 1 equiv.) and hydrazine monohydrate (0.3 mL, 0.2 g, 4 mmol, 1.3 equiv.) in methanol (50 mL) was heated to reflux. The reaction was monitored by TLC until completion (3 h). Aqueous sodium hydroxide (20 mL, 30%) was added and the resulting mixture was concentrated and extracted with dichloromethane (3 × 50 mL). The organic extracts were combined, washed with brine (20 mL), dried with sodium sulfate, filtered and concentrated to provide the corresponding hydrazone. The hydrazone was directly dissolved in chloroform (100 mL), after which activated manganese dioxide (0.8 g, 9.1 mmol, 2.8 equiv.) was added. The heterogeneous mixture was heated at reflux overnight. The resulting mixture was cooled to 25 °C and filtered over celite. After concentration, **15** was obtained as a brown solid (1 g, 91%); m.p. 180–182 °C. ^{1}H NMR (300 MHz, $CDCl_3$): δ = 8.82 (d, *J* = 8.4 Hz, 1 H, 9 H), 8.49 (d, *J* = 9.3 Hz, 1 H, 4-H), 8.35 (dd, *J* = 7.8, 0.8 Hz, 1 H, 3′-H), 7.89 (dd, *J* = 7.9, 1.1 Hz, 1 H, 6-H), 7.79 (ddd, *J* = 8.5, 7.3, 1.4 Hz, 1 H, 8-H), 7.7–7.6 (m, 3 H, 4′-H, 5-H, 7-H), 7.41 (dd, *J* = 7.8, 0.8 Hz, 1 H, 5′-H) ppm. ^{13}C NMR (75.5 MHz, $CDCl_3$, 25 °C): δ = 152.7 (C), 141.5 (C), 139.0 (CH), 1376 (C), 131.8 (C), 130.3 (C), 130.2 (CH), 128.6 (CH), 128.1 (CH), 127.4 (CH), 126.1 (CH), 124.4 (C), 119.2 (CH), 117.5 (CH), 116.4 (CH) ppm. MS (EI): *m*/*z* (%) = 326 (14), 324 (15), 298 (80), 296 (79), 217 (100), 216 (50), 190 (33), 128 (18). HRMS (EI) calcd. for $C_{15}H_9{}^{79}BrN_4$: 324.0011; found 324.0012. HRMS (EI) calcd. for $C_{15}H_9{}^{81}BrN_4$: 326.0011; found 326.0000. Elemental analysis (%) calcd. for $C_{15}H_9BrN_4$: C 55.40, H 2.79, N 17.23; found C 55.34, H 3.24, N 17.05.

3-(6-Methylpyridin-2-yl)[1,2,3]triazolo[1,5-*a*]quinoline (16): Butyllithium (0.4 mL, 0.7 mmol, 1.1 equiv.) in hexanes (1.5 M) was added at –78 °C to a solution of **15** (0.2 g, 0.6 mmol, 1.0 equiv.) in tetrahydrofuran (20 mL). The mixture was kept for 30 min at –78 °C, after which iodomethane (0.1 g, 0.8 mmol, 1.2 equiv.) was added. The mixture was allowed to warm to room temperature in the course of 1 h. Saturated aqueous ammonium chloride (20 mL) was added and the resulting mixture was extracted with dichloromethane (3 × 50 mL). The organic extracts were combined, washed with brine (10 mL), dried with sodium sulfate, filtered and concentrated. Chromatography (silica gel, ethyl acetate/cyclohexane, 1:4) provided **16** (81 mg, 50%); m.p. 116–117 °C. ^{1}H NMR (300 MHz, $CDCl_3$, 25 °C): δ = 8.83 (d, *J* = 8.4 Hz, 1 H, 9-H), 8.59 (d, *J* = 9.3 Hz, 1 H, 4-H), 8.20 (d, *J* = 7.9 Hz, 1 H, 3′-H), 7.87 (dd, *J* = 7.9, 1.1 Hz, 1 H, 6-H), 7.77 (ddd, *J* = 8.5, 7.4, 1.4 Hz, 1 H, 8-H), 7.70 (t, *J* = 7.8, 7.8 Hz, 1 H, 4′-H), 7.6–7.5 (m, 2 H, 5-H, 7-H), 7.10 (d, *J* = 7.6 Hz, 1 H, 5′-H), 2.66 (s, 3 H, CH_3) ppm. ^{13}C NMR

(75.5 MHz, $CDCl_3$, 25 °C): δ = 158.0 (C), 151.3 (C), 139.3 (C), 136.9 (CH), 131.9 (C), 130.0 (C), 129.9 (CH), 128.4 (CH), 127.2 (CH), 127.1 (CH), 124.4 (C), 121.6 (CH), 118.1 (CH), 117.7 (CH), 116.4 (CH), 29.7 (CH_3) ppm. MS (EI): *m*/*z* (%) = 260 (16), 232 (100), 231 (58). HRMS (EI) calcd. for $C_{16}H_{12}N_4$: 260.1062; found 260.1064.

Supporting Information (see also the footnote on the first page of this article): ^1H, ^{13}C NMR spectra for compounds **2**–**16**, and computational data.

Acknowledgments

This work was carried out with financial support from the Ministerio de Educación y Ciencia (MEC) (Projects CTQ2007–61901/BQU and CTQ2006–15672-C05–03), the Comunidad Autónoma de Madrid (Project MADRISOLAR, ref. S-0505/PPQ/0225) and the French Centre National de la Recherche Scientifique (CNRS). Thanks are given to the CTI (Consejo Superior de Investigaciones Científicas, CSIC) and CESGA for allocation of computer time. R. B. G. is much indebted to the French Ministère de l'Éducation Nationale, de la Recherche et de la Technologie for a doctoral fellowship.

[1] B. Abarca-González, *J. Enzyme Inhib. Med. Chem.* **2002**, *17*, 359–367.
[2] F. Blanco, I. Alkorta, J. Elguero, V. Cruz, B. Abarca, R. Ballesteros, *Tetrahedron* **2008**, *64*, 11150–11158.
[3] B. Abarca, I. Alkorta, R. Ballesteros, F. Blanco, M. Chadlaoui, J. Elguero, M. Mojarrad, *Org. Biomol. Chem.* **2005**, *3*, 3905–3910.
[4] B. Abarca, R. Ballesteros, M. Chadlaoui, *Tetrahedron* **2004**, *60*, 5785–5792.
[5] G. Jones, D. R. Sliskovic, *J. Chem. Soc. Perkin Trans. 1* **1982**, 967–971.
[6] G. Jones, D. R. Sliskovic, *Tetrahedron Lett.* **1980**, *21*, 4529–4530.
[7] S. Chuprakov, F. W. Hwang, V. Gevorgyan, *Angew. Chem. Int. Ed.* **2007**, *46*, 4757–4759.
[8] a) H. C. v. d. Plas, *Ring Transformation of Heterocycles*. Academic, London. **1973**; b) R. E. Valters, W. Flitsch, *Ring-Chain Tautomerism*, Plenum, New York, **1985**.
[9] a) R. E. Valters, F. Fulop, D. Korbonits, *Adv. Heterocycl. Chem.* **1995**, *64*, 251–321; b) R. E. Valters, F. Fulop, D. Korbonits, *Adv. Heterocycl. Chem.* **1996**, *66*, 1–71; c) L. Lazar, F. Fulop, *Eur. J. Org. Chem.* **2003**, 3025–3042.
[10] B. Abarca, R. Ballesteros, M. Elmasnauoy, *Tetrahedron* **1999**, *55*, 12881–12884.
[11] R. Ballesteros-Garrido, L. Bonnafoux, B. Abarca, F. R. Leroux, F. Colobert, *Dalton Trans.* **2009**, 5068–5070.
[12] B. Abarca, R. Aucejo, R. Ballesteros, F. Blanco, E. Garcia-España, *Tetrahedron Lett.* **2006**, *47*, 8101–8103.
[13] F. Colobert, R. Ballesteros-Garrido, F. R. Leroux, R. Ballesteros, B. Abarca, *Tetrahedron Lett.* **2007**, *48*, 6896–6899.
[14] B. Abarca, R. Ballesteros, R. Ballesteros-Garrido, F. Colobert, F. R. Leroux, *Tetrahedron* **2007**, *63*, 10479–10485.
[15] B. Abarca, R. Ballesteros, R. Ballesteros-Garrido, F. Colobert, F. R. Leroux, *Tetrahedron* **2008**, *64*, 3794–3801.
[16] R. Ballesteros-Garrido, F. R. Leroux, R. Ballesteros, B. Abarca, C. Ramirez de Arellano, F. Colobert, E. Garcia-España, *New J. Chem.*, in press.
[17] B. Abarca, E. G. Aldavari, G. Jones, *J. Chem. Res. (S)* **1984**, 140–141.
[18] B. Abarca, R. Ballesteros, E. G. Aldavari, G. Jones, *J. Chem. Soc. Perkin Trans. 1* **1985**, 1897–1901.
[19] B. Abarca, R. Ballesteros, N. Houari, *Tetrahedron* **1997**, *53*, 12765–12770.
[20] R. Ballesteros-Garrido, F. R. Leroux, R. Ballesteros, B. Abarca, F. Colobert, *Tetrahedron* **2009**, *65*, 4410–4417.
[21] B. Abarca, R. Ballesteros, M. Elmasnaouy, *Tetrahedron* **1998**, *54*, 15287–15292.
[22] CCDC-739144 contains the supplementary crystallographic data for this paper. These data can be obtained free of charge from The Cambridge Crystallographic Data Centre via www.ccdc.cam.ac.uk/data_request/cif.
[23] I. Rozas, I. Alkorta, J. Elguero, *J. Phys. Chem. A* **1998**, *102*, 9925–9932.
[24] J. R. Bartels-Keitanhd, R. W. Cieciuch, *Can. J. Chem.* **1968**, *46*, 2593–2600.
[25] C. T. Lee, W. T. Yang, R. G. Parr, *Phys. Rev. B* **1988**, *37*, 785–789.
[26] A. D. Becke, *J. Chem. Phys.* **1993**, *98*, 5648–5652.
[27] M. J. Frisch, G. W. Trucks, H. B. Schlegel, G. E. Scuseria, M. A. Robb, J. R. Cheeseman, J. A. Montgomery, T. Vreven, K. N. Kudin, J. C. Burant, J. M. Millam, S. S. Iyengar, J. Tomasi, V. Barone, B. Mennucci, M. Cossi, G. Scalmani, N. Rega, G. A. Petersson, H. Nakatsuji, M. Hada, M. Ehara, K. Toyota, R. Fukuda, J. Hasegawa, M. Ishida, T. Nakajima, Y. Honda, O. Kitao, H. Nakai, M. Klene, X. Li, J. E. Knox, H. P. Hratchian, J. B. Cross, V. Bakken, C. Adamo, J. Jaramillo, R. Gomperts, R. E. Stratmann, O. Yazyev, A. J. Austin, R. Cammi, C. Pomelli, J. W. Ochterski, P. Y. Ayala, K. Morokuma, G. A. Voth, P. Salvador, J. J. Dannenberg, V. G. Zakrzewski, S. Dapprich, A. D. Daniels, M. C. Strain, O. Farkas, D. K. Malick, A. D. Rabuck, K. Raghavachari, J. B. Foresman, J. V. Ortiz, Q. Cui, A. G. Baboul, S. Clifford, J. Cioslowski, B. B. Stefanov, G. Liu, A. Liashenko, P. Piskorz, I. Komaromi, R. L. Martin, D. J. Fox, T. Keith, M. A. Al-Laham, C. Y. Peng, A. Nanayakkara, M. Challacombe, P. M. W. Gill, B. Johnson, W. Chen, M W. Wong, C. Gonzalez, J. A. Pople, *Gaussian 03*, Gaussian, Inc., Wallingford, CT, **2003**.
[28] R. F. W. Bader, *Atoms in Molecules: A Quantum Theory*, Clarendon Press, Oxford, **1990**.
[29] F. W. Biegler-König, J. Schönbom, *AIMM2000, A program to analyze and visualize atoms in molecules*, v. 2.0, Bielefeld, Germany, **2002**.

Received: July 21, 2009
Published Online: October 7, 2009

